Supplement of Atmos. Chem. Phys., 21, 11053–11068, 2021
https://doi.org/10.5194/acp-21-11053-2021-supplement

Atmospheric Chemistry and Physics
Open Access
EGU

Supplement of

Development of ozone reactivity scales for volatile organic compounds in a Chinese megacity

Yingnan Zhang et al.

Correspondence to: Likun Xue (xuelikun@sdu.edu.cn)

1. Field observations

Field observations were conducted from 1 January 2018 to 31 December 2019 at the Guangzhou Environmental Monitoring Center Station (23.12° N, 113.27° E, 51 m above sea level). It is a typical urban site located at Jixiang Road, Yuexiu District of Guangzhou, an urban area surrounded by massive residential and commercial buildings. The pillar industries are business industry, financial industry, cultural creativity industry, and health care over the area, therefore, the site is mainly subjected to traffic emissions and rarely impacted by industrial source. The site is set up on the rooftop of an eight-floor building with an altitude of ~40 m above the ground level and the data collected here can reflect urban pollution characteristics.

Real-time measurements of trace gases, including O_3, NO, NO_2, CO, SO_2, and VOCs were implemented using standard commercial techniques. O_3 was measured by a UV photometric ozone analyzer (Thermo 49i) with a detection limit of 0.50 ppbv. NO and NO_2 were monitored using a chemiluminescence analyzer (Thermo 42i) with a detection limit of 0.40 ppbv. CO was measured by a gas filter correlation, non-dispersive infrared analyzer (Thermo 48i) with a detection limit of 40 ppbv. SO_2 was measured by a pulsed fluorescence gas analyzer (Thermo 43i) with a detection limit of 1 ppbv. The quality assurance and quality control procedures were implemented according to "Technical Specifications for Automatic Monitoring of Ambient Air Quality (HJT193-2005)". VOCs were measured using the GC866 online analyzer (Chromatotec) with a detection limit of 0.01 ppbv. The detection system consists of two analyzers: the low-carbon analyzer is responsible for the collection and detection of C_2-C_6 hydrocarbons, and the high-carbon analyzer is responsible for the collection and detection of C_6-C_{12} hydrocarbons. Both analyzers use flame ionization detector for detection, and totally 57 hydrocarbons (specified by the Photochemical Assessment Monitoring Stations of US Environmental Protection Agency (USEPA)) were detected. Meteorological parameters including ambient temperature, relative humidity (RH), and pressure were obtained from a commercial meteorological station (Vaisala, Finland).

2. Model configuration

The model was run based on the platform of F0AM (Framework for 0-D Atmospheric Modeling) (Wolfe et al., 2016), and the adopted chemical mechanism was the state-of-the-art Master Chemical Mechanism version 3.3.1 (MCMv3.3.1), which near-explicitly describes the atmospheric degradation of 143 VOC species and has been extensively used to elucidate the non-linear photochemistry between O_3 and its precursors (NOx and VOCs) (Chen et al., 2020; Xue et al., 2014). In addition to the comprehensive chemistry, the model also considers several physical processes, including solar radiation, diurnal evolution of the PBL, dry deposition, and dilution with background air (Chen et al., 2019; Xue et al., 2014; Xue et al., 2013; Edwards et al., 2014). The solar radiation was calculated as a function of solar zenith angle under the assumption of clear sky conditions. The PBL height was

parameterized to rise linearly from the minimum height of 300 m at 06:00 LT to the maximum height of 1500 m at 14:00 LT, kept constant at its maximum in the afternoon, and then set to its minimum at 20:00 LT. Dry deposition velocities of a series of organic and inorganic molecules were parameterized based on the work of Zhang et al. (2003).

The dilution with background air was parameterized according to the work of Edwards et al. (2014). The dilution constant of air exchange with background air was assumed to be 1.16×10^{-5} s^{-1} during the first simulation, then the model was iteratively run to obtain more reasonable dilution constant according to:

$$CONS_{i+1} = CONS_i * (CO_{obs}/CO_i) \quad (1)$$

where CO_i and $CONS_i$ represent the simulated CO concentration and adopted dilution constant in the i^{th} simulation, respectively, and CO_{obs} refers to the observed concentration of CO. Background concentrations of pollutants were set according to previous studies in the PRD and Hong Kong (see SI Table S1 for background concentrations) (Guo et al., 2013; Li et al., 2013; Li et al., 2018). The VOCs without available background concentrations were set as 0.05 ppbv.

3. Emission inventory

For the emission-based inputs, the emissions of NOx, SO_2, CO, and Non-methane VOCs (NMVOCs) were set as medians of emissions within grid cells contained in urban Guangzhou. Here we considered two types of primary emission sources: biogenic emissions and anthropogenic emissions. The biogenic emissions (for isoprene, β-pinene, and limonene) were derived based on MERRA-2 (www.pku-atmos-acm.org/; 0.5° × 0.625°; monthly resolution in 2017; Weng et al., 2020). The anthropogenic emissions were derived from the MEIC inventory (Multi-resolution Emission Inventory for China; 0.25° × 0.25°; monthly resolution in 2016; http://www.meicmodel.org/; Li et al., 2014; Li et al., 2019). For anthropogenic NOx emission, a ratio of 9:1 was used to allocate it into NO and NO_2. The emission profile of individual NMVOC species from a given anthropogenic emission sector was obtained from previous studies and the USEPA SPECIATE 4.5 database (Li et al., 2014; Liu et al., 2008a; Liu et al., 2008b; Tsai et al., 2003; Wang et al., 2009; Zheng et al., 2009). The real-time emission rate (unit: molecules cm^{-3} s^{-1}) of a specific pollutant was calculated as follows. The species profile of each emission sector was first multiplied by its total emissions, the emission rate was then calculated assuming that the pollutants were well mixed within the planetary boundary layer (except for biogenic VOCs whose diurnal pattern was determined according to temperature), and the final emission rate of the specific pollutant was summed from anthropogenic and biogenic sources.

4. Uncertainty evaluation

We conducted a series of sensitivity tests to evaluate the uncertainties introduced by the VOC initialization treatment with emission-based inputs. The sensitivity tests were designed by changing

the initial concentrations of individual selected compound or all compounds without available observational data. The individual compound who is either the most reactive or the most unreactive within major sub-groups was selected (i.e., ethanol, 1,3-dimethyl-5-ethyl, 2-methyl-2-butene, *i*-butene, and methyl glyoxal) to better reflect the effects of VOCs with different chemical characteristics on O_3 formation. For the sensitivity tests targeted at individual selected compound, the initial concentrations of ethanol, 1,3-dimethyl-5-ethyl, 2-methyl-2-butene, *i*-butene, and methyl glyoxal were set as 10, 2, 1.5, 1.5, and 1.5 ppbv, respectively (named as "ADJ1", "ADJ2", "ADJ3", "ADJ4", and "ADJ5", respectively, in Table S5). For the sensitivity tests targeted at all compounds without available observational data, the initial concentrations of these VOC species were set as 0.50 ppbv (named as "ADJ6" in Table S5). The comparison results showed that the MIR and MOR scales (especially ranks) were relatively insensitive to the VOC initialization treatment (as indicated by the strong R^2 (0.98-1.00) and the slopes (0.80-1.04)).

Figures & Tables

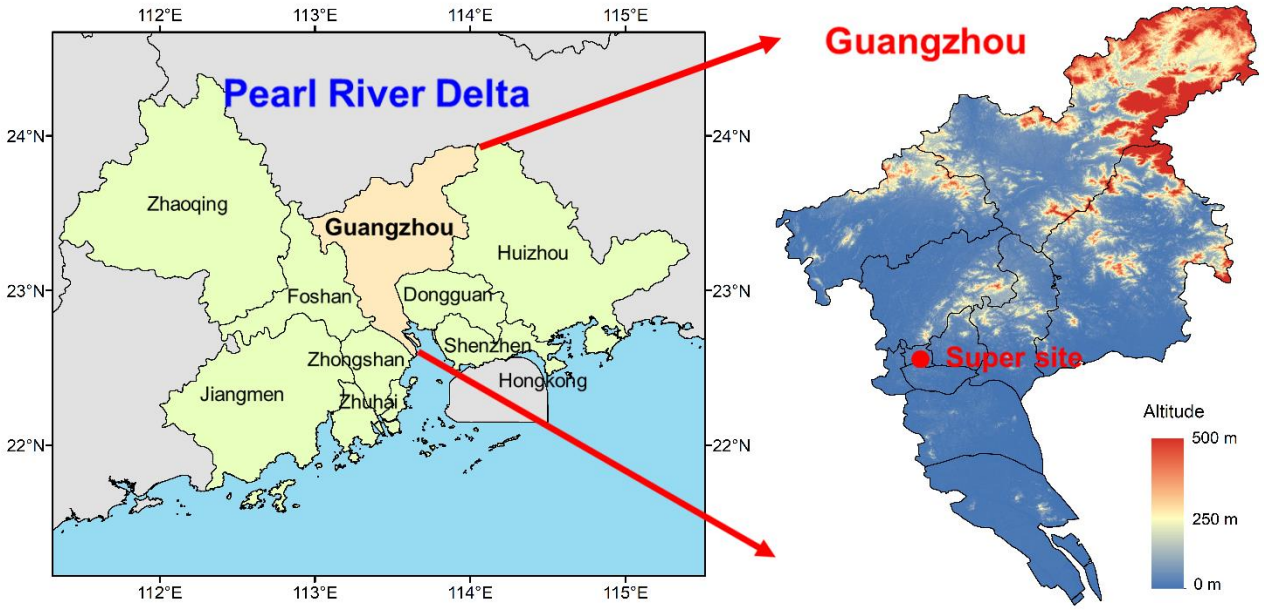

Figure S1. Map showing the locations of the Pearl River Delta region, Guangzhou, and the study site at urban Guangzhou.

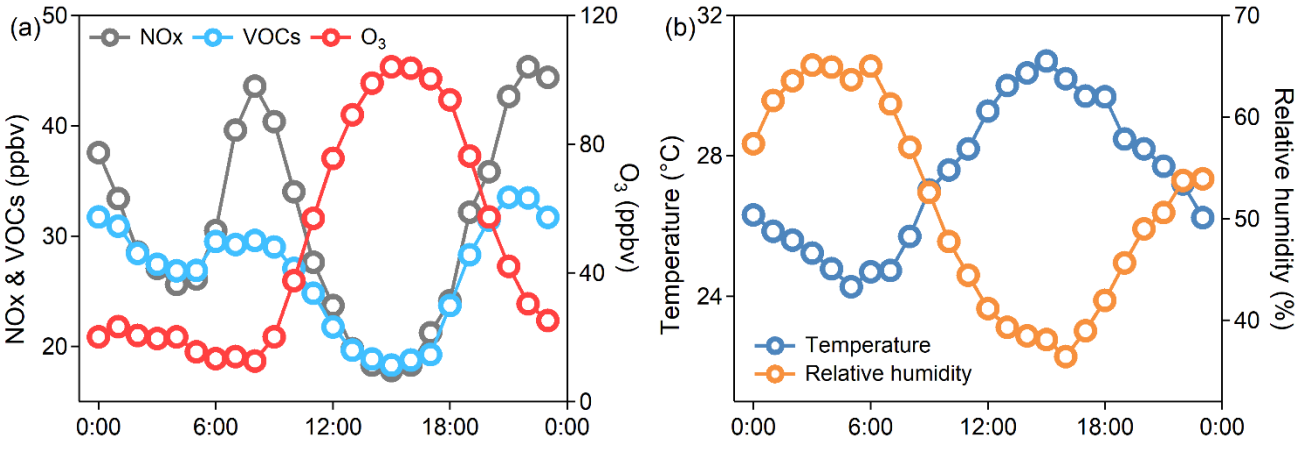

Figure S2. Diurnal variations of (a) NOx, VOCs, O_3, and (b) meteorological parameters for the observation-based inputs. The data were medians of 67 selected non-attainment days when maximum daily 8-h average O_3 mixing ratio exceeded the Chinese National Ambient Air Quality Standard, i.e., 75 ppbv (Class II) at an urban site in Guangzhou during 2018-2019.

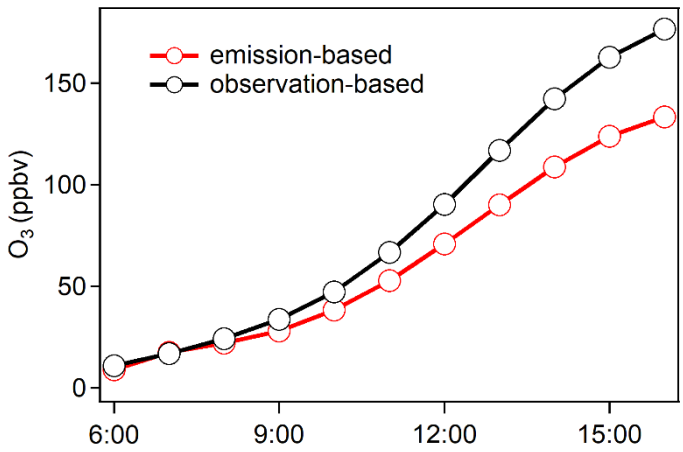

Figure S3. The model-simulated O_3 concentrations with emission-based and observation-based inputs during the 10-h integral period.

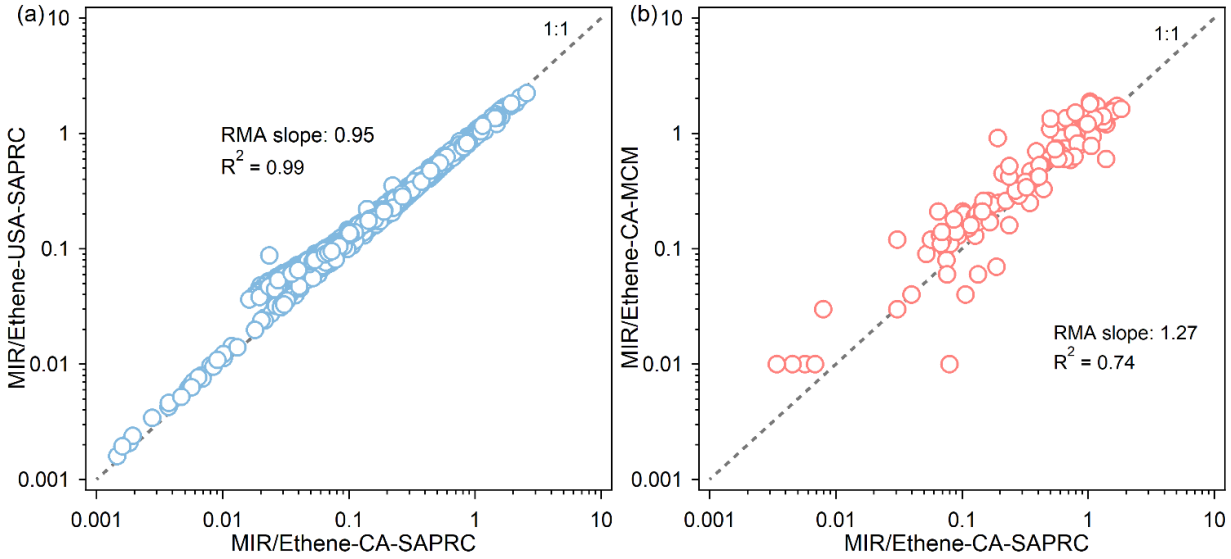

Figure S4. Comparison of MIR/Ethene scales obtained from California scenarios using SAPRC-07 mechanism against (a) those obtained from the U.S. scenarios using SAPRC-07 mechanism and (b) those obtained from California scenarios using MCM. The panels are shown in log scales, and only positively reactive VOCs are shown. The grey dashed line represents 1:1 line. Data of MIR/Ethene-CA-SAPRC and MIR/Ethene-USA-SAPRC are taken from Carter et al. (2010) and data of MIR/Ethene-CA-MCM are taken from Derwent et al. (2010).

Table S1. Descriptive statistics of chemical species and meteorological parameters observed during the 67 O_3 episodes days (units: pptv unless otherwise specified).

Species	Mean ± stdev	Median	Species	Mean ± stdev	Median
O_3 (ppbv)	52 ± 38	44	*n*-undecane	41 ± 35	30
CO (ppbv)	934 ± 337	928	*n*-dodecane	64 ± 57	50
NO_2 (ppbv)	30.0 ± 17.2	25.3	1-butene	128 ± 142	90

NO (ppbv)	8.0 ± 16.4	3.0	ethene	1797 ± 1514	1410
SO_2 (ppbv)	4.4 ± 1.3	4.2	propene	315 ± 294	220
ethyne	1738 ± 819	1550	*cis*-2-butene	87 ± 70	60
ethane	1774 ± 1506	1410	*trans*-2-butene	69 ± 51	50
propane	5603 ± 5116	4360	*1*-pentene	37 ± 28	30
n-butane	3165 ± 2385	2630	isoprene	687 ± 989	360
i-butane	1708 ± 1296	1420	benzene	364 ± 254	270
n-pentane	821 ± 680	610	toluene	2060 ± 1707	1620
i-pentane	1335 ± 968	1120	ethyl benzene	467 ± 454	335
2,2-dimethyl butane	41 ± 29	30	*m*-xylene	1028 ± 1196	670
2,3-dimethyl butane	267 ± 435	50	styrene	106 ± 183	50
2-methyl pentane	315 ± 319	180	*o*-xylene	512 ± 469	380
3-methyl pentane	274 ± 172	230	*i*-propyl benzene	24 ± 38	20
n-hexane	377 ± 287	320	*n*-propyl benzene	27 ± 20	20
3-methyl hexane	318 ± 299	230	*o*-ethyl toluene	39 ± 29	30
n-heptane	252 ± 297	160	*m*-ethyl toluene	98 ± 92	70
n-octane	439 ± 371	330	1,3,5-trimethyl benzene	46 ± 47	30
n-nonane	41 ± 51	30	T (°C)	27.7 ± 3.7	27.8
n-decane	73 ± 90	50	RH (%)	49 ± 14	48

104

Table S2a. Detailed input data for the base case emission-based inputs (Hr-*X* represents local time).

Input of chemical species											
Species	Initial (ppbv)	Emission rate (10^{-10} mol m^{-3} h^{-1})									
		Hr-6	Hr-7	Hr-8	Hr-9	Hr-10	Hr-11	Hr-12	Hr-13	Hr-14	Hr-15	Hr-16
NMVOCs	38	1271	2135	2135	2135	1386	1305	1213	1197	1191	1183	1166
NOx	30	1218	2046	2046	2046	1328	1250	1162	1147	1141	1134	1117
SO_2	5	315	530	530	530	344	324	301	297	295	294	289
CO	918	6027	10123	10123	10123	6568	6185	5751	5675	5643	5609	5528
Isoprene	0.3	4	4	3	5	6	7	8	8	8	8	7
O_3	13	Calculate maximum O_3: 133 ppbv										
Input of meteorological parameters												
Parameter		Hr-6	Hr-7	Hr-8	Hr-9	Hr-10	Hr-11	Hr-12	Hr-13	Hr-14	Hr-15	Hr-16
PBL height (m)		300	349	527	706	884	1063	1241	1420	1500	1500	1500
Temperature (deg K)		297.4	297.9	297.9	298.9	300.2	300.8	301.4	302.4	303.2	303.5	303.9
Relative humidity (%)		65	61	57	53	48	44	41	39	38	38	36
Dilution rate ($10^{\wedge-6}$ s^{-1})		7.54	4.83	2.44	2.47	4.80	10.91	24.70	24.71	22.26	19.75	19.76

Table S2b. The same as Table 2a but for the base case observation-based inputs.

Input of chemical species											
Species	Constrained concentration (ppbv)										
	Hr-6	Hr-7	Hr-8	Hr-9	Hr-10	Hr-11	Hr-12	Hr-13	Hr-14	Hr-15	Hr-16
NMVOCs	38	37	38	37	35	33	29	27	26	26	27
NOx	30	40	44	40	34	28	24	20	18	18	18
SO_2	5	4	5	5	5	5	5	4	4	4	4
CO	918	960	1023	1041	1000	942	876	864	859	854	842
Isoprene	0.3	0.4	0.3	0.5	0.6	0.7	0.8	0.8	0.8	0.8	0.6
O_3	13	Calculate maximum O_3: 177 ppbv									
Input of meteorological parameters											
Parameter	Hr-6	Hr-7	Hr-8	Hr-9	Hr-10	Hr-11	Hr-12	Hr-13	Hr-14	Hr-15	Hr-16
PBL height (m)	300	349	527	706	884	1063	1241	1420	1500	1500	1500
Temperature (deg K)	297.4	297.9	297.9	298.9	300.2	300.8	301.4	302.4	303.2	303.5	303.9
Relative humidity (%)	65	61	57	53	48	44	41	39	38	38	36
Dilution rate ($10^{\wedge-6}$ s^{-1})	7.54	4.83	2.44	2.47	4.80	10.91	24.70	24.71	22.26	19.75	19.76

Table S2c. The same as Table 2a but for the U.S. "averaged conditions" scenario. The data are taken from Carter (1994).

Input of chemical species											
Species	Initial (ppbv)	Emission rate (10^{-10} mol m^{-3} h^{-1})									
		Hr-1	Hr-2	Hr-3	Hr-4	Hr-5	Hr-6	Hr-7	Hr-8	Hr-9	Hr-10
NMVOCs	780	1227	760	500	288	194	171	146	126	127	135
NOx	90	1559	970	624	389	285	244	222	200	197	198
SO_2	-	-	-	-	-	-	-	-	-	-	-
CO	2028	25852	15838	10261	5976	3177	2732	2400	2122	2194	2376
Isoprene	0.1	39	52	67	67	75	75	72	74	67	54
O_3	-	Calculate maximum O_3: 206 ppbv									
Input of meteorological parameters											
Parameter	Hr-0	Hr-1	Hr-2	Hr-3	Hr-4	Hr-5	Hr-6	Hr-7	Hr-8	Hr-9	Hr-10
PBL height (m)	293	596	899	1201	1503	1610	1716	1823	1823	1823	1823
Temperature (deg K)	295.5	297.7	299.9	301.8	303.3	304.5	305.6	305.8	306.1	305.9	305.0
H_2O ($10^{\wedge 4}$ ppm)	1.994	2.040	2.059	2.036	2.029	1.991	1.888	1.854	1.899	1.997	2.033

Table S3. Detailed parameters setup for emission-based inputs.

Species	Initial concentration (ppbv)	Background concentration (ppbv)	Anthropogenic NMVOC emission factor (%)	Group
CO	918	330	-	-
O_3	13	80	-	-
NO_2	28	3	-	-
NO	3	0.20	-	-
HONO	0.61	0.20	-	-
SO_2	5	1.50	-	-
acrolein	0.10	0.05	0.05	OVOC
benzaldehyde	0.10	0.05	0.16	OVOC
benzene	0.28	0.30	5.05	Aromatic
biacetyl	0.10	0.05	0.02	OVOC
2-butoxy-ethanol	0.10	0.05	0.45	OVOC
1-butene	0.30	0.05	0.99	Alkene
sec-butyl alcohol	0.10	0.05	0.06	OVOC
ethyne	1.47	0.50	1.00	Alkyne
ethene	1.65	0.40	6.58	Alkene
propionaldehyde	0.10	0.05	0.13	OVOC
ethanol	0.10	0.10	2.46	OVOC
ethane	1.55	0.50	2.28	Alkane
propene	0.50	0.05	3.50	Alkene
butanal	0.10	0.05	0.08	OVOC
propane	4.98	0.50	2.98	Alkane
3-methylbutanal	0.10	0.05	0.00	OVOC
crotonaldehyde	0.10	0.05	0.11	OVOC
1,3-butadiene	0.10	0.05	0.61	Alkene
pentanal	0.10	0.05	0.01	OVOC
hexanal	0.10	0.05	0.02	OVOC
heptanal	0.10	0.05	0.02	OVOC
benzyl alcohol	0.10	0.05	< 0.01	OVOC
cis-2-butene	0.30	0.05	0.14	Alkene
dichloromethane	0.10	0.05	0.15	Halocarbon
1,1,1-trichloroethane	0.10	0.05	0.21	Halocarbon
acetaldehyde	0.30	0.05	0.63	OVOC
acetic acid	0.10	0.05	0.01	OVOC
acetone	0.10	0.05	0.90	OVOC
dimethyl ether	0.10	0.05	< 0.01	OVOC
methanol	0.10	0.05	0.16	OVOC
1,1-dichloroethane	0.10	0.05	< 0.01	Halocarbon
cyclohexane	0.10	0.05	0.42	Alkane
cis-2-hexene	0.10	0.05	0.02	Alkene
cis-2-pentene	0.10	0.05	0.08	Alkene
cyclohexanone	0.10	0.05	0.02	OVOC
diethyl ether	0.10	0.05	0.03	OVOC
1,3-dimethyl-5-ethyl benzene	0.10	0.05	0.17	Aromatic
dimethoxy methane	0.10	0.05	1.78	OVOC
ethyl benzene	0.40	0.05	1.99	Aromatic
2-ethoxy-ethanol	0.10	0.05	0.01	OVOC
ethyl acetate	0.10	0.05	0.15	OVOC
diethylene glycol	0.10	0.05	0.09	OVOC
ethylene oxide	0.10	0.05	0.00	OVOC
glyoxal	0.10	0.05	0.09	OVOC
formaldehyde	0.50	0.05	1.01	OVOC
formic acid	0.10	0.05	< 0.01	OVOC
1-hexene	0.10	0.05	0.15	Alkene
2-hexanone	0.10	0.05	0.03	OVOC
hexanol	0.10	0.05	< 0.01	OVOC
i-butyl alcohol	0.10	0.05	< 0.01	OVOC
i-butane	1.80	0.05	3.16	Alkane

i-pentane	1.39	0.14	1.05	Alkane
i-propyl benzene	0.20	0.05	0.06	Aromatic
2-methyl propanal	0.10	0.05	0.01	OVOC
i-propyl acetate	0.10	0.05	0.08	OVOC
i-propyl alcohol	0.10	0.05	0.59	OVOC
2,2-dimethyl butane	0.40	0.05	0.11	Alkane
2,3-dimethyl butane	0.82	0.05	0.32	Alkane
5-methyl-2-hexanone	0.10	0.05	< 0.01	OVOC
2-methyl hexane	0.10	0.05	0.05	Alkane
2-methyl pentane	0.46	0.05	0.36	Alkane
4-methyl-2-pentanol	0.10	0.05	< 0.01	OVOC
3-methyl hexane	0.32	0.05	0.18	Alkane
3-methyl pentane	0.32	0.05	0.22	Alkane
methacrolein	0.10	0.05	0.02	OVOC
2-methyl-1-butene	0.10	0.05	0.03	Alkene
2-methyl-2-butene	0.10	0.05	0.15	Alkene
3-methyl-1-butene	0.10	0.05	0.05	Alkene
methyl ethyl ketone	0.10	0.05	0.84	OVOC
i-butene	0.10	0.05	0.37	Alkene
methyl acetate	0.10	0.05	< 0.01	OVOC
m-ethyl toluene	0.35	0.05	0.41	Aromatic
*m*ethyl glyoxal	0.10	0.05	0.04	OVOC
4-methyl-2-pentanone	0.10	0.05	1.08	OVOC
methyl tert-butyl ether	0.10	0.05	0.09	OVOC
m-xylene	0.94	0.05	4.84	Aromatic
3-Methylbenzaldehyde	0.10	0.05	0.02	OVOC
n-butyl acetate	0.10	0.05	1.30	OVOC
n-butyl alcohol	0.10	0.05	1.38	OVOC
n-decane	0.30	0.05	1.24	Alkane
n-undecane	0.30	0.05	0.67	Alkane
n-dodecane	0.50	0.05	0.16	Alkane
n-butane	3.24	0.20	3.16	Alkane
n-pentane	0.90	0.05	1.32	Alkane
n-hexane	0.51	0.05	2.39	Alkane
n-heptane	0.34	0.05	2.92	Alkane
n-octane	0.36	0.05	1.95	Alkane
n-nonane	0.30	0.05	1.05	Alkane
propyl acetate	0.10	0.05	0.86	OVOC
n-propyl alcohol	0.10	0.05	< 0.01	OVOC
3-octanol	0.10	0.05	< 0.01	OVOC
o-ethyl toluene	0.30	0.05	0.64	Aromatic
o-xylene	0.40	0.05	2.06	Aromatic
2-Methylbenzaldehyde	0.10	0.05	0.01	OVOC
2,3-dimethyl phenol	0.10	0.05	< 0.01	OVOC
n-propyl benzene	0.20	0.05	0.57	Aromatic
1-pentene	0.30	0.05	0.09	Alkene
p-ethyl toluene	0.10	0.05	0.15	Aromatic
acetophenone	0.10	0.05	0.03	OVOC
phenol	0.10	0.05	0.03	OVOC
1-methoxy-2-propanol	0.10	0.05	0.06	OVOC
propylene glycol	0.10	0.05	0.01	OVOC
p-xylene	0.10	0.05	1.21	Aromatic
4-methylbenzaldehyde	0.10	0.05	0.07	OVOC
styrene	0.30	0.05	3.25	Aromatic
trans-2-butene	0.30	0.05	0.08	Alkene
trans-2-hexene	0.10	0.05	0.05	Alkene
1,2,3-trimethyl benzene	0.25	0.05	0.84	Aromatic
1,2,4-trimethyl benzene	0.30	0.05	0.88	Aromatic
1,3,5-trimethyl benzene	0.20	0.05	0.54	Aromatic
toluene	1.50	0.48	10.79	Aromatic
trans-2-pentene	0.10	0.05	0.10	Alkene

vinyl chloride	0.10	0.05	0.64	Halocarbon
β-pinene	0.10	0.05	-	Alkene
isoprene	0.30	0.05	-	Alkene
limonene	0.10	0.05	-	Alkene

Table S4. Correlations of IR/Ethene scales under MIR and MOR scenarios for 116 VOC species between base case emission-based inputs and sensitivity scenarios. The base IR/Ethene scales were used as benchmarks (*x*-axis). Six sensitivity scenarios: (1) ADJ1: the initial concentration of ethanol increased to 10 ppbv, while other factors were kept unchanged; (2) ADJ2: the initial concentration of 1,3-dimethyl-5-ethyl increased to 2 ppbv, while other factors were kept unchanged; (3) ADJ3: the initial concentration of 2-methyl-2-butene increased to 1.5 ppbv, while other factors were kept unchanged; (4) ADJ4: the initial concentration of *i*-butene increased to 1.5 ppbv, while other factors were kept unchanged; (5) ADJ5: the initial concentration of methyl glyoxal increased to 1.5 ppbv, while other factors were kept unchanged; (6) ADJ6: the initial concentrations of VOCs without available observational data were set as 0.50 ppbv, while other factors were kept unchanged.

MIR/Ethene			MOR/Ethene		
Scenarios	RMA slope	R^2	Scenarios	RMA slope	R^2
ADJ1	1.03	1.00	ADJ1	1.03	1.00
ADJ2	0.95	1.00	ADJ2	0.92	1.00
ADJ3	0.89	0.99	ADJ3	0.92	0.99
ADJ4	0.96	1.00	ADJ4	0.97	1.00
ADJ5	0.86	0.99	ADJ5	0.89	0.99
ADJ6	0.88	0.98	ADJ6	0.89	0.99

Table S5a. Dependence of emission–based MIR/Ethene scales for major VOC groups on major environmental conditions. The base MIR/Ethene scales were used as benchmarks (*x*-axis). Eight sensitivity scenarios: (2) 0.25*VOCs: both initial and emitted VOCs multiplied by 0.25, while other factors were kept unchanged, (3)-(6) *X**VOC group: both initial and emitted VOC species contained in the target VOC group multiplied by *X*, and other VOC compositions increased or decreased to keep VOCs/NOx ratios constant, while other factors were kept unchanged, (7) HONO: both initial and emitted HONO were set to zero, and only the gas phase formation pathway (OH + NO = HONO) of HONO was included in the model, (8) 0.5*J: the photolysis rate was reduced to a half, while other factors were kept unchanged, (9) 3 days: the model integration time lasted for 3 days, while other factors were kept unchanged. Refer to Table S3 for the detailed speciation of VOCs.

VOC group	0.25*VOCs		0.25*OVOCs		1.5*Alkanes		2*Aromatics		2*Alkenes		HONO		0.5*J		3 days	
	RMA slope	R^2	RMA slope	R^2	RMA slope	R^2	RMA slope	R^2	RMA slope	R^2	RMA slope	R^2	RMA slope	R^2	RMA slope	R^2
Aldehydes	0.90	0.99	1.12	1.00	1.21	1.00	1.07	1.00	0.89	1.00	1.10	1.00	1.62	0.98	0.73	0.83
Alkanes	1.04	0.99	1.01	1.00	1.06	0.99	0.99	1.00	0.98	1.00	1.00	1.00	1.17	0.92	1.11	0.43
Alkenes	0.77	0.97	1.14	1.00	1.16	1.00	1.19	0.99	0.86	0.99	1.14	1.00	1.64	0.97	0.46	0.64
Aromatics	1.02	1.00	1.03	1.00	1.07	1.00	0.93	1.00	0.97	1.00	1.00	1.00	1.21	0.98	0.73	0.95
TVOC	0.91	0.99	1.09	1.00	1.15	1.00	1.05	0.99	0.92	1.00	1.07	1.00	1.46	0.97	0.72	0.81

Table S5b. The same as Table S5a but for MOR/Ethene scales.

VOC group	0.25*VOCs		0.25*OVOCs		1.5*Alkanes		2*Aromatics		2*Alkenes		HONO		0.5*J		3 days	
	RMA slope	R^2	RMA slope	R^2	RMA slope	R^2	RMA slope	R^2	RMA slope	R^2	RMA slope	R^2	RMA slope	R^2	RMA slope	R^2
Aldehydes	1.00	0.99	1.09	1.00	1.29	0.99	0.92	1.00	0.89	1.00	1.11	1.00	1.68	0.95	0.36	0.01
Alkanes	1.06	0.98	1.01	1.00	1.06	0.97	0.96	0.98	0.99	0.99	0.99	1.00	1.18	0.81	1.10	0.31
Alkenes	0.87	0.98	1.07	1.00	1.23	0.98	1.02	0.99	0.87	0.98	1.13	0.99	1.72	0.91	0.71	0.06
Aromatics	1.07	1.00	1.02	1.00	1.11	1.00	0.89	1.00	0.96	1.00	1.01	1.00	1.19	0.98	0.62	0.80
TVOC	0.99	0.99	1.06	1.00	1.21	0.99	0.94	1.00	0.91	1.00	1.08	1.00	1.50	0.97	0.48	0.42

References

Carter, W. P. L.: Calculation of Reactivity Scales Using an Updated Carbon Bond IV Mechanism, Report Prepared for Systems Applications Internation for the Auto/Oil Air Quality Improvement Program., 1994.

Chen, T., Xue, L., Zheng, P., Zhang, Y., Liu, Y., Sun, J., Han, G., Li, H., Zhang, X., Li, Y., Li, H., Dong, C., Xu, F., Zhang, Q., and Wang, W.: Volatile organic compounds and ozone air pollution in an oil production region in northern China, Atmos. Chem. Phys., 20, 7069-7086, 10.5194/acp-20-7069-2020, 2020.

Edwards, P. M., Brown, S. S., Roberts, J. M., Ahmadov, R., Banta, R. M., deGouw, J. A., Dubé, W. P., Field, R. A., Flynn, J. H., Gilman, J. B., Graus, M., Helmig, D., Koss, A., Langford, A. O., Lefer, B. L., Lerner, B. M., Li, R., Li, S.-M., McKeen, S. A., Murphy, S. M., Parrish, D. D., Senff, C. J., Soltis, J., Stutz, J., Sweeney, C., Thompson, C. R., Trainer, M. K., Tsai, C., Veres, P. R., Washenfelder, R. A., Warneke, C., Wild, R. J., Young, C. J., Yuan, B., and Zamora, R.: High winter ozone pollution from carbonyl photolysis in an oil and gas basin, Nature, 514, 351-354, 10.1038/nature13767, 2014.

Guo, H., Ling, Z. H., Cheung, K., Jiang, F., Wang, D. W., Simpson, I. J., Barletta, B., Meinardi, S., Wang, T. J., Wang, X. M., Saunders, S. M., and Blake, D. R.: Characterization of photochemical pollution at different elevations in mountainous areas in Hong Kong, Atmos. Chem. Phys., 13, 3881-3898, 10.5194/acp-13-3881-2013, 2013.

Li, M., Zhang, Q., Streets, D. G., He, K. B., Cheng, Y. F., Emmons, L. K., Huo, H., Kang, S. C., Lu, Z., Shao, M., Su, H., Yu, X., and Zhang, Y.: Mapping Asian anthropogenic emissions of non-methane volatile organic compounds to multiple chemical mechanisms, Atmos. Chem. Phys., 14, 5617-5638, 10.5194/acp-14-5617-2014, 2014.

Li, M., Zhang, Q., Zheng, B., Tong, D., Lei, Y., Liu, F., Hong, C., Kang, S., Yan, L., Zhang, Y., Bo, Y., Su, H., Cheng, Y., and He, K.: Persistent growth of anthropogenic non-methane volatile organic compound (NMVOC) emissions in China during 1990–2017: drivers, speciation and ozone formation potential, Atmos. Chem. Phys., 19, 8897-8913, 10.5194/acp-19-8897-2019, 2019.

Li, X., Brauers, T., Hofzumahaus, A., Lu, K., Li, Y. P., Shao, M., Wagner, T., and Wahner, A.: MAX-DOAS measurements of NO_2, HCHO and CHOCHO at a rural site in Southern China, Atmos. Chem. Phys., 13, 2133-2151, 10.5194/acp-13-2133-2013, 2013.

Li, Z., Xue, L., Yang, X., Zha, Q., Tham, Y. J., Yan, C., Louie, P. K. K., Luk, C. W. Y., Wang, T., and Wang, W.: Oxidizing capacity of the rural atmosphere in Hong Kong, Southern China, Sci. Total Environ., 612, 1114-1122, https://doi.org/10.1016/j.scitotenv.2017.08.310, 2018.

Liu, Y., Shao, M., Fu, L., Lu, S., Zeng, L., and Tang, D.: Source profiles of volatile organic compounds (VOCs) measured in China: Part I, Atmos. Environ., 42, 6247-6260, https://doi.org/10.1016/j.atmosenv.2008.01.070, 2008a.

Liu, Y., Shao, M., Lu, S., Chang, C.-C., Wang, J.-L., and Fu, L.: Source apportionment of ambient

volatile organic compounds in the Pearl River Delta, China: Part II, Atmos. Environ., 42, 6261-6274, https://doi.org/10.1016/j.atmosenv.2008.02.027, 2008b.

Tsai, S. M., Zhang, J., Smith, K. R., Ma, Y., Rasmussen, R. A., and Khalil, M. A. K.: Characterization of Non-methane Hydrocarbons Emitted from Various Cookstoves Used in China, Environ. Sci. Technol., 37, 2869-2877, 10.1021/es026232a, 2003.

Wang, S., Wei, W., Du, L., Li, G., and Hao, J.: Characteristics of gaseous pollutants from biofuel-stoves in rural China, Atmos. Environ., 43, 4148-4154, https://doi.org/10.1016/j.atmosenv.2009.05.040, 2009.

Weng, H.-J., Lin, J.-T., Martin, R., Millet, D. B., Jaeglé, L., Ridley, D., Keller, C., Li, C., Du, M.-X., and Meng, J.: Global high-resolution emissions of soil NOx, sea salt aerosols, and biogenic volatile organic compounds, Sci. Data, 7, 148, doi:10.1038/s41597-020-0488-5, 2020, 2020.

Wolfe, G. M., Marvin, M. R., Roberts, S. J., Travis, K. R., and Liao, J.: The Framework for 0-D Atmospheric Modeling (F0AM) v3.1, Geosci. Model Dev., 9, 3309-3319, 10.5194/gmd-9-3309-2016, 2016.

Xue, L., Wang, T., Gao, J., Ding, A. J., Zhou, X. H., Blake, D. R., Wang, X. F., Saunders, S. M., Fan, S. J., Zuo, H. C., Zhang, Q. Z., and Wang, W. X.: Ground-level ozone in four Chinese cities: precursors, regional transport and heterogeneous processes, Atmos. Chem. Phys., 14, 13175-13188, 10.5194/acp-14-13175-2014, 2014.

Xue, L. K., Wang, T., Guo, H., Blake, D. R., Tang, J., Zhang, X. C., Saunders, S. M., and Wang, W. X.: Sources and photochemistry of volatile organic compounds in the remote atmosphere of western China: results from the Mt. Waliguan Observatory, Atmos. Chem. Phys., 13, 8551-8567, 10.5194/acp-13-8551-2013, 2013.

Zhang, L., Brook, J. R., and Vet, R.: A revised parameterization for gaseous dry deposition in air-quality models, Atmos. Chem. Phys., 3, 2067-2082, 10.5194/acp-3-2067-2003, 2003.

Zheng, J., Shao, M., Che, W., Zhang, L., Zhong, L., Zhang, Y., and Streets, D.: Speciated VOC Emission Inventory and Spatial Patterns of Ozone Formation Potential in the Pearl River Delta, China, Environ. Sci. Technol., 43, 8580-8586, 10.1021/es901688e, 2009.